ISET Journal of Earthquake Technology, Paper No. 594, Vol. 62, No. 1, March 2025, pp. 59-77

LATERAL FLOW IN RECLAIMED LAND DUE TO LIQUEFACTION DURING THE 2024 NOTO PENINSULA EARTHQUAKE, JAPAN~ INSIGHTS FROM REMOTE SENSING AND FIELD SURVEY ~

Hemanta Hazarika (Corresponding Author)
Professor, Kyushu University, E mail id: hazarika@civil.kyushu-u.ac.jp

Shiro Ohta
Head, Planning and Technology Division, Kawasaki Geological Engineering Co., Ltd., E mail id: ohtas@kge.co.jp

Shotaro Kubota
Sub Leader, Planning and Technology Division, Kawasaki Geological Eng. Co., Ltd., E mail id: kubotas@kge.co.jp

Yuji Michi
Senior Managing Director, Yoshimitsugumi Inc., E mail id: michi@yoshimitsugumi.co.jp

Anurag Sahare
Research Assistant Professor, Tokyo City University, E mail id: sahare@tcu.ac.jp

Tsuyoshi Tanaka
Technical Officer, Tokyo City University, E mail id: ttanaka@tcu.ac.jp

Tomohiro Ishizawa
Chief Researcher, National Research Institute for Earth Science and Disaster Resilience
E mail id: ishizawa@bosai.go.jp

Masanori Murai
Senior Engineer, Shimizu Corporation, E mail id: m.murai@shimz.co.jp

Takashi Fujishiro
President, Geo Disaster Prevention Institute, E mail id: fujishiro.jibanbousai@gmail.com

Tatsunori Matsumoto
Professor Emeritus, Kanazawa University, E mail id: matsumototatsunori55@gmail.com

Taichi Hyodo
Lecturer, Toyama Prefectural University, E mail id: t.hyodo@pu-toyama.ac.jp

ABSTRACT

On January 1, 2024, at 16:10 JST, a powerful earthquake with a moment magnitude of 7.5 struck the Noto Peninsula in southeastern Japan, with the epicenter in Suzu City, Ishikawa Prefecture. The earthquake brought extensive devastation to the prefectures of Ishikawa, Fukui, Toyama, and Niigata. Low-rise buildings, roads, utilities, port facilities, and other essential infrastructures sustained significant damage. Slope and embankment failures disrupted the transportation network on the Noto Peninsula, hampering the recovery efforts. The earthquake also triggered severe soil liquefaction, leading to widespread geotechnical and structural damage. Liquefaction was not limited to coastal areas near the epicenter; it was observed in more distant parts of Ishikawa Prefecture and in the neighboring prefectures as well. The town of Uchinada, Ishikawa Prefecture, with its gently sloped reclaimed land, was particularly hard hit, with significant lateral spreading causing massive damage to low-rise buildings, roads, and public utilities. To better understand the mechanism behind the widespread liquefaction and its associated damage in Uchinada Town, a joint investigation team comprising researchers and engineers from academia, government, and industry was formed a month after the earthquake. The team conducted several surveys in Uchinada Town and nearby areas between February and August 2024. This paper presents the detailed findings of the investigation, along with a factorial analysis of the extensive lateral displacement that caused damage to infrastructures.

KEYWORDS: Later Flow; Liquefaction; Remote Sensing; Field Survey

https://doi.org/10.63898/WWTQ3912

INTRODUCTION

A strong earthquake struck the Noto Peninsula located south-east of Japan with the epicenter in Suzu City, Ishikawa Prefecture on January 1, 2024, at 16:10 JST causing widespread damage in the prefectures of Ishikawa, Fukui, Toyama and Niigata. According to the data reported by the Japan Meteorological Agency (JMA), this earthquake exhibited JMA magnitude Mj of 7.6 (moment magnitude MW of 7.5) with a focal depth of approximately 16 km and is characterized by a reverse fault mechanism with a northwest-southeast compression axis (JMA, 2024). According to JMA, the earthquake was preceded by a foreshock with a magnitude of 5.7 and was succeeded by 8582 aftershocks with the largest one having a magnitude of 6.1. The main shock inflicted widespread damage on low-rise houses, roads, utilities, port facilities, and other vital infrastructure. Slope and embankment failures have crippled the transportation network on the Noto Peninsula, creating significant obstacles to recovery efforts. The earthquake also triggered a tsunami, with waves reaching heights of up to 6.58 meters along the Sea of Japan coast.

The earthquake was Japan's deadliest, since the 2011 Great East Japan Earthquake, claiming 412 lives and injuring 1,300 people (Fire and Disaster Management Agency, 2024). A total of 168,822 structures were damaged, with the Japanese government estimating the economic loss at $17.6 billion USD. Approximately 90% of the casualties were caused by falling debris from severely damaged buildings. In Wajima City, the earthquake ignited a massive fire that destroyed 200 buildings, including the Asaichi morning market and a shopping district. In Suzu, the epicenter of the earthquake, about 90% of the buildings sustained damage, particularly wooden structures, which were hit hardest.

The earthquake resulted in severe soil liquefaction and multiple landslides, causing widespread geotechnical damage not only in Ishikawa Prefecture, but also in nearby prefectures. Figure 1 shows the areas affected by soil liquefaction and landslides during the earthquake.

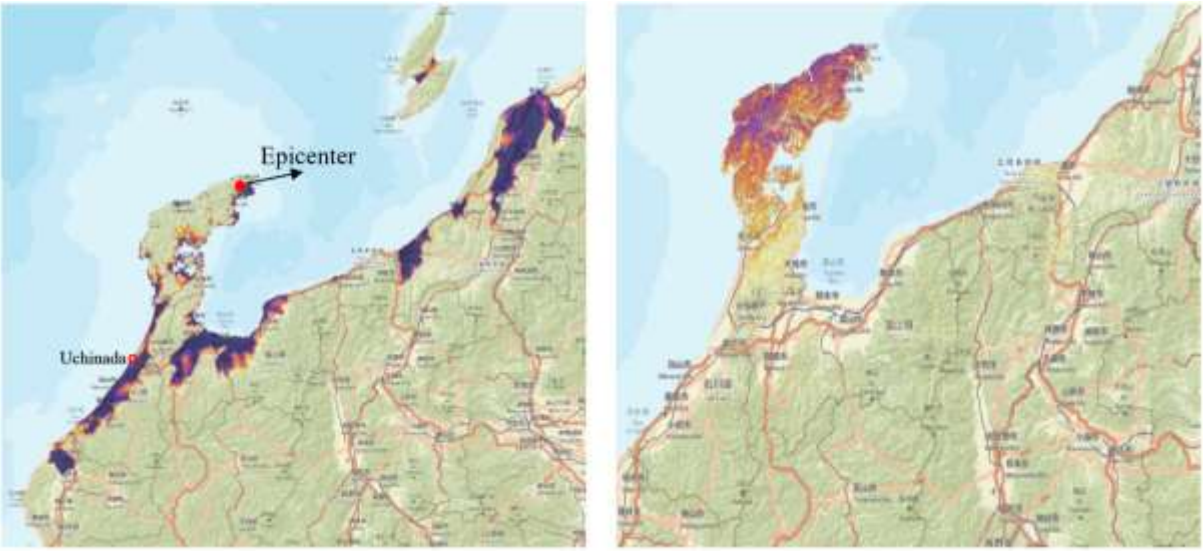

(a) Liquefaction induced damage (b) Landslides induced damage

Fig. 1 Areas affected by the soil liquefaction and landslides due to the 2024 Noto Peninsula earthquake (source: USGS)

The occurrences of liquefaction were not confined solely to the coastal areas near the epicenter; it was also observed in distant regions such as Uchinada Town located 100 km to the south of the epicenter, including nearby Toyama Prefecture located 60 km to the southeast and Fukui Prefecture, located 200 km to the southwest, as well as Niigata Prefecture located 160 km to the Northeast of the epicenter. As seen in Figure 1(a), damage due to soil liquefaction was particularly evident near the Uchinada Town in Ishikawa Prefecture. Significant liquefaction-induced lateral spreading was reported because of the presence of sand dunes with a gentle slope in Uchinada Town. This widespread distribution of liquefaction phenomena underscores the extensive impact of the earthquake. While local ground conditions played a role in the observed effects, one of the factors driving such widespread liquefaction was the significant ground motion produced by the rupture of a fault approximately 130 km long.

To investigate the mechanism behind the widespread liquefaction and the resulting damage to low-rise buildings, infrastructures, and public utilities, a joint team of researchers and engineers from academia, government, and industry was formed under the leadership of the first author. The team conducted several surveys at the Uchinada Town from February 2024 until August 2024 and reported the results of the preliminary investigations (Fujishiro et al., 2024; Hazarika et al., 2024; Hu et al., 2024; Kubota et al., 2024a, 2024b, 2024c; Michi et al., 2024; Murai et al., 2024; Sahare et al., 2024). This paper presents the detailed investigation results and factorial analysis of the significant lateral displacement of structures through two case studies.

EARTHQUAKE MECHANISM AND GROUND MOTION CHARACTERISTICS

1. Earthquake Mechanism

The 2024 Noto Peninsula Earthquake, with its epicenter located in the northern part of the Noto Peninsula, was characterized by its substantial magnitude and extensive spatial impact. Figure 2 presents the epicentral distribution of the mainshock and subsequent aftershocks, as derived from the analysis conducted by the National Research Institute for Earth Science and Disaster Resilience (NIED, 2024b). The main shock and its aftershocks were distributed over approximately 150 km from the southwest to the northeast of the Noto Peninsula. Particularly notable seismic activity was observed in the region extending from Wajima City to Suzu City.

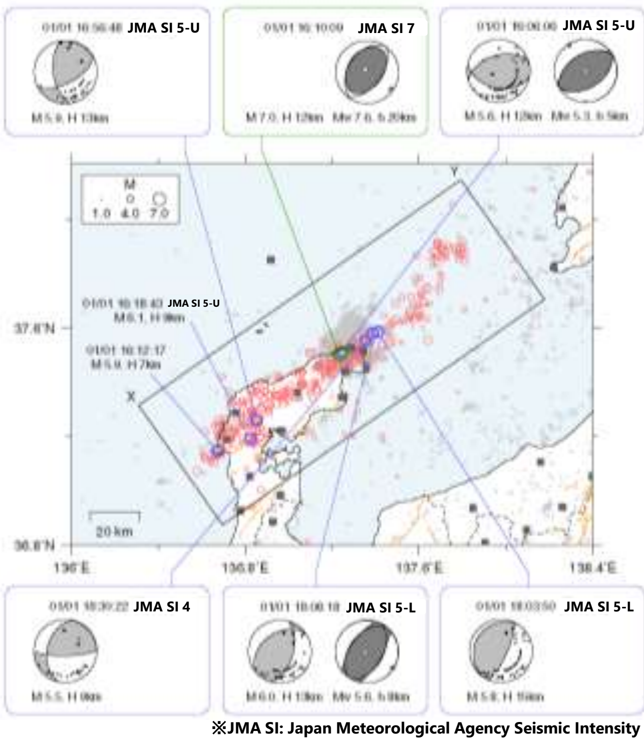

Fig. 2 Epicentral distribution of the 2024 Noto Peninsula Earthquake mainshock and aftershocks (NIED, 2024b)

Figure 3 illustrates the results of source inversion analysis utilizing strong-motion waveform records, performed by NIED (2024a). Figure 3 (a) shows the surface projection of the final slip distribution on the fault plane, while Figure 3 (b) depicts the slip distribution on the fault plane itself. The estimated fault plane model consists of three rectangular fault planes. The rupture process analysis revealed significant rupture in the shallow regions northeast (fault plane #1) and southwest (fault planes #2 and #3) of the rupture initiation point. The rupture process exhibited a complex temporal evolution. Initially, no significant rupture was observed for approximately 15 seconds after the onset. Subsequently, the shallow region of fault plane #2 began to rupture, followed by the initiation of rupture in the shallow areas of fault plane #1 and #3 at approximately 30 seconds after the onset. The maximum slip was estimated to be 5.3 m.

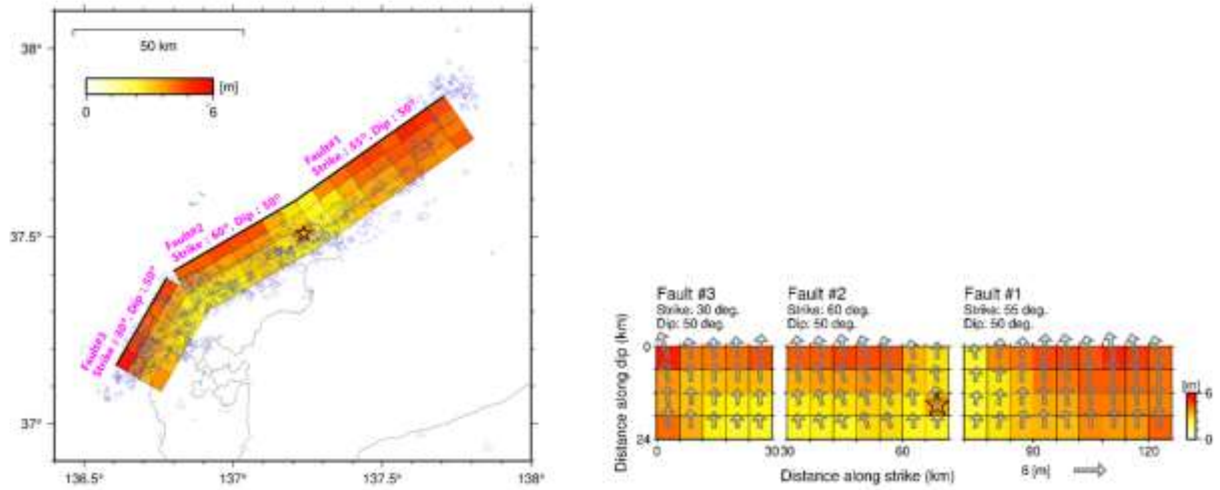

(a) Surface projection of slip distribution (b) Slip distribution on the fault plane

Fig. 3 Source inversion analysis results using strong-motion waveform records by NIED (2024a)

2. Ground Motion Characteristics

One of the distinctive features of this seismic event was its prolonged ground motion duration which resulted in extensive damage over a wide area. As reported by the JMA (2024), seismic intensities of 7 on JMA scale was recorded in Wajima City and Shika Town near the epicenter. The tremors were felt across a wide area, with seismic intensity of 1 recorded as far as Hokkaido in northern Japan and Kyushu region in the south. The Noto Peninsula, in proximity to the epicenter, experienced intensities ranging from 7 to 6-Lower, while an intensity of 6-Lower was recorded in Nagaoka City, Niigata Prefecture, located approximately 140 km southeast of the epicenter.

Figure 4 illustrates the distribution of Peak Ground Acceleration (PGA) at various strong-motion stations within the NIED's strong-motion seismograph network (NIED, 2024a) during the mainshock of the earthquake. The Figure also delineates the epicenter, estimated fault model, locations of slope failures, and areas affected by liquefaction. The slope failure data was derived from the deposition distribution dataset provided by the Geospatial Information Authority of Japan (GSI, 2024). Liquefaction occurrence sites were extracted according to the report by Senna (2024).

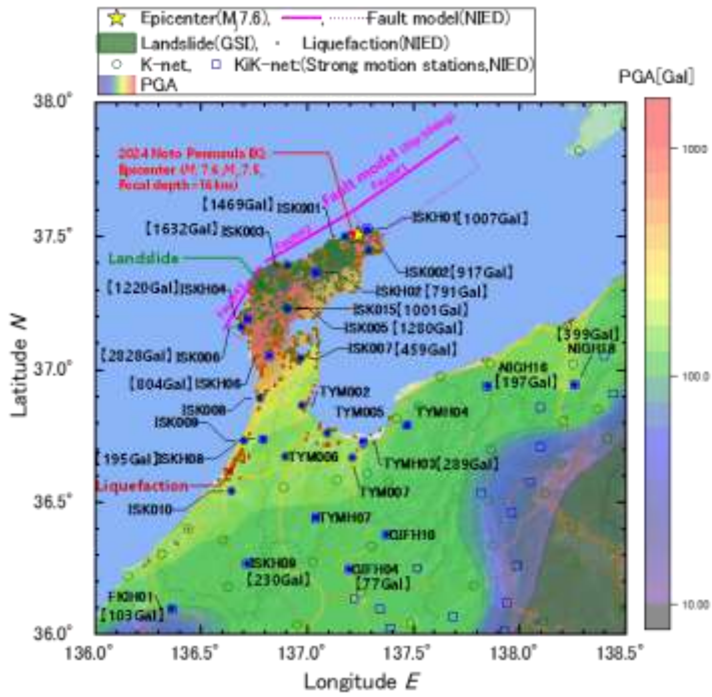

Fig. 4 Distribution of Peak Ground Acceleration (PGA) during the mainshock, slope failures and liquefied areas

Notably, seven sites near the source fault in Suzu City, Wajima City, Anamizu Town, and Shika Town in the Ishikawa Prefecture recording values exceeding 1000 Gal (where Gal = cm/s²). Among these, the K-NET Togi station (ISK006) recorded a significantly high PGA of 2828 Gal, the magnitude being very close to the PGA of 2933 Gal observed during the 2011 Great East Japan Earthquake (Mw 9.0). Although PGA alone does not fully characterize shaking intensity, the high PGA values corresponded with widespread structural damage near the fault. Numerous building collapses were reported, and frequent slope failures were observed, particularly closer to the fault planes #2 and #3, southwest of the epicenter.

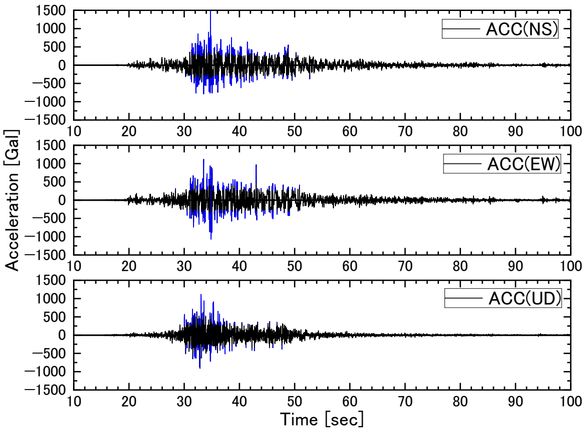

Fig. 5 Strong-motion record from K-NET Wajima (ISK003)

Figure 5 presents the strong-motion record (PGA = 1632 Gal) from the K-NET Wajima (ISK003), a location that experienced substantial building damage, liquefaction, and landslides. The Figure demonstrates that high accelerations (e.g., exceeding ±250 Gal) persisted for over 15 seconds. This duration is notably longer compared to inland earthquakes of similar magnitude. The source inversion analysis reveals a characteristic rupture process involving stepwise and widespread propagation. This unique rupture mechanism likely caused the observed prolonged strong shaking across an extensive area.

Table 1 summarizes the characteristics of 11 strong-motion stations located near the fault. These stations were located at the epicentral distances ranging from 2 to 60 km and exhibited surface S-wave velocities between 90 and 440 m/s. In the near-fault region, no clear correlation was observed between epicentral distance and PGA or Peak Ground Velocity (PGV).

Table 1: Characteristics of strong-motion stations near the fault

Strong motion station (K-NET, KiK-net)		**Epicenter distance R0 (km)**	**S-wave velocity V_s (m/s)**	**Peak ground acceleration PGA (cm/s² = Gal)**	**Peak ground velocity PGV (cm/s)**
ISK006	Togi	59	260	2828	84
ISK003	Wajima	28	230	1632	104
ISK001	Ohtani	2	200	1469	110
ISK005	Amamizu	40	120	1280	149
ISKH04	Togi	55	440	1220	85
ISKH01	Suzu	8	240	1007	148
ISK015	Ohmachi	40	120	1001	105
ISK002	Syoin	10	110	917	137
ISKH06	Shika	60	240	804	45
ISKH02	Yanagida	21	420	791	64
ISK007	Nanao	55	90	459	33

TOPOGRAPHY, GEOLOGY AND HISTORY OF RECLAMATION IN UCHINADA TOWN

Coastal sand dunes have formed along the coastline of the Kaga region in Ishikawa Prefecture, stretching from the Komatsu Plain to the north. These dunes are distributed in the following order: the

Daishoji Dunes, the Komatsu Dunes, the Yasuhara Dunes, and the Uchinada Dunes (Fuji, 1971). The Uchinada Dunes are transverse dunes, approximately 1.5 km wide, extending from Awagasaki Town in Kanazawa City to Hidono in Kahoku City. The highest point of the dunes reaches an elevation of 60 meters, with an average height of 20 meters. The slopes are gentle on the seaward side and steep on the inland side as depicted in Figure 6.

The region from Ohsaki in Kahoku City to Miyasaka in Uchinada Town is located on the southeastern side (the reclaimed land side) of sand dunes, which were linearly formed in a northeast-southwest direction, with an elevation of about 50 meters. The reclaimed land was once a brackish lake called Kahoku Lagoon, where small-scale land reclamation began in the Edo period. Large-scale reclamation work was carried out under the National Kahoku Lagoon Land Reclamation Project starting in 1963, and the land was fully reclaimed in 1971. During the reclamation, the sand from the dunes was extensively excavated, and according to past topographic maps, areas that were once dune slopes were transformed into flat residential land due to the reclamation as shown in Figure 7.

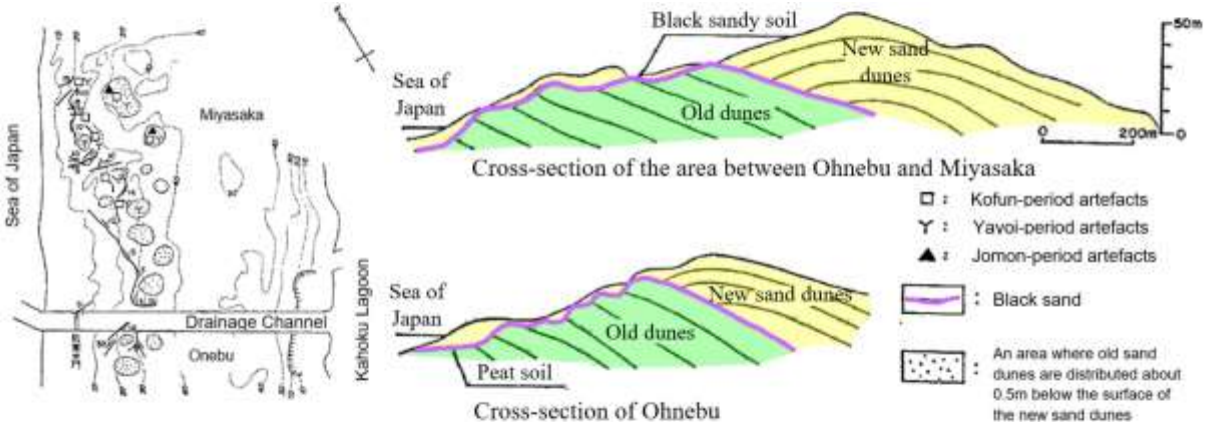

Fig. 6 Cross sectional view of Uchinada sand dunes (Southern area), Ishikawa Prefecture (After Fuji, 1971)

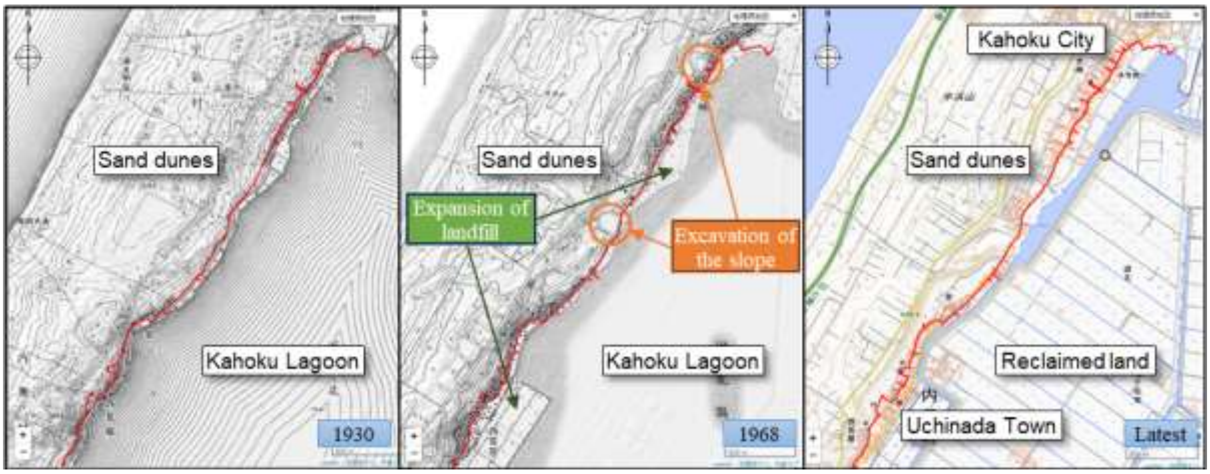

Fig. 7 Topographic change from Ohsaki (Kahoku City) to Miyasaka (Uchinada Town)

DAMAGE DUE TO LIQUEFACTION IN UCHINADA TOWN

In the region extending from Ōhsaki in Kahoku City to Miyasaka in Uchinada Town, significant ground deformation has been observed, particularly along the base of the sand dune slopes near Prefectural Road 8, where it has occurred continuously in a belt-like pattern as shown in Figure 8. Soil liquefaction has led to the formation of sand boils, resulting in uneven settlement and ground uplift that have caused many buildings to tilt or sink. Additionally, retaining walls have collapsed or shifted, road pavements have been damaged and raised, and utility poles have visibly tilted. In some areas, blockages in waterways have also been noted. Many residents have been forced to evacuate their homes, which were no longer habitable. Examples of the ground deformation and associated damage are illustrated in Figures 9-12.

Our investigation revealed that ground subsidence and uplift occur in tandem, characterized by multiple parallel subsidence lines, which are interpreted as tension cracks. Uplift has taken place on the lower side of these subsidence lines (on the reclaimed land side), forming along the compression axis in the same direction as the slope of the ground. Above the subsidence lines (on the sand dunes side), there is minimal ground deformation. However, between the subsidence and uplift zones, prominent features include sand boils, ground settlement, and the tilting of structures. The compression axis of the tension cracks and uplift aligns in a northeast-southwest direction along the dune ridge. Based on these observations, it could be concluded that the subsidence and uplift are the result of ground failure caused by lateral movement induced by liquefaction.

An example of ground deformation due to lateral movement at Sakakibara Shrine in Ohsaki, Kahoku City, along with a schematic cross-section, is shown in Figure 13. It appears that a slope failure due to lateral flow occurred on a gently sloping area with a gradient of approximately 3 degrees and a height difference of around 2 meters. Interestingly, the Prefectural Road 8 at the base of the slope dune avoided collapse due to liquefaction induced lateral flow, rather it prevented the flow from the west side of the road and the road was uplifted due to compression and experienced horizontal bending in several places.

Fig. 8. Location map of severe liquefaction area

Fig. 9 Houses in the Ohsaki area of Kahoku City (Uplift of road and lateral movement of houses in the reclaimed land)

(a) Water channel blockage (b) 12 m of lateral displacement of residential building

Fig. 10 Blockage of water channel and lateral movement of a building in Muro area

(a) Pile supported undamaged house in Muro (b) Differential settlement in Miyasaka

Fig. 11 Performance of good foundation and bad foundation during liquefaction

(a) Subsidence of the front of school building (b) Uplifting of the road

Fig. 12 Building and road damage due to liquefaction in Nishi Araya area

(a) Area location

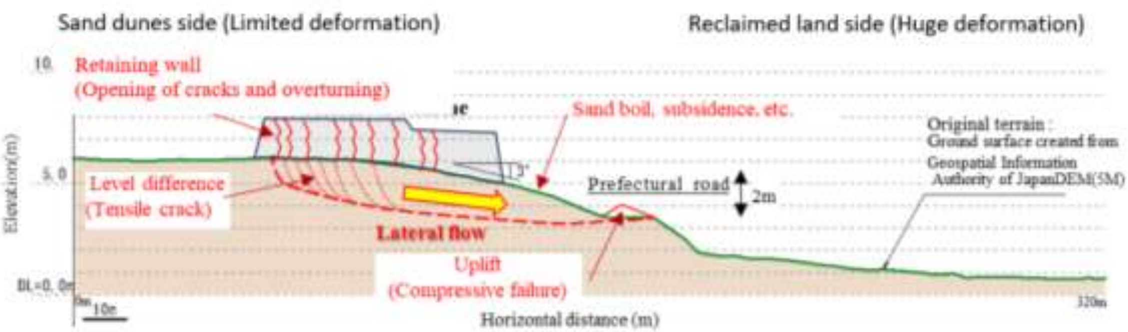

(b) Schematic cross section

Fig. 13 Lateral flow near Sakakibara shrine in Ohsaki area (Kahoku City)

REMOTE SENSING AND FIELD TESTING IN THE LIQUIFIED AREA

1. Location of the Surveyed Area

In order to understand the geological and geotechnical characteristics and liquefaction potential of the area, ground investigations were conducted in the Nishi Araya and Muro districts of Uchinada Town (Figure 14), where severe liquefaction and lateral flow induced damage were confirmed during our preliminary survey.

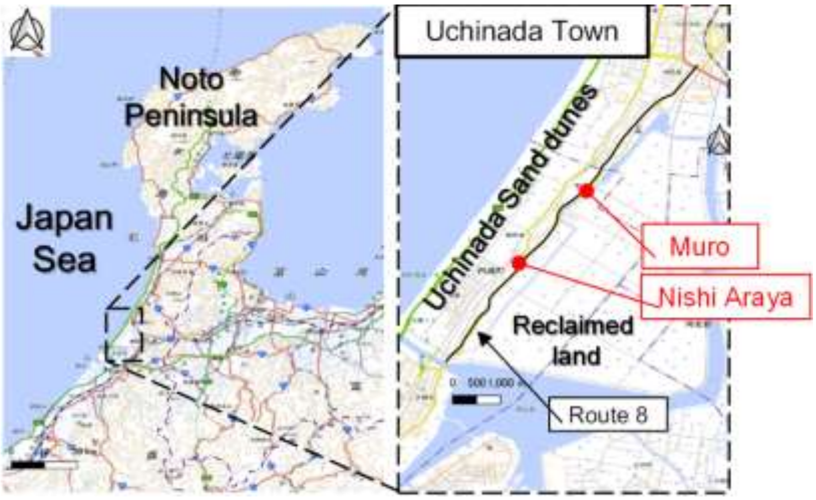

Fig. 14 Location map of the surveyed area

Fig. 15 Historical aerial photograph of the Nishi Araya area (After Tani, 2016)

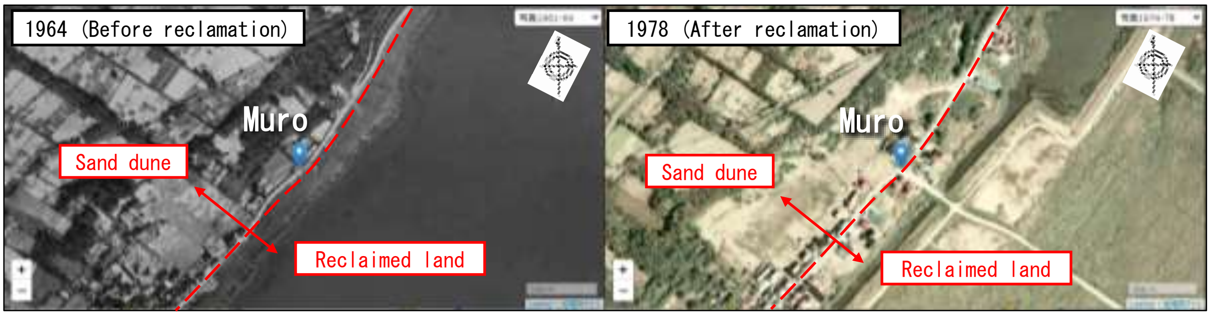

Fig. 16 Historical aerial photograph of the Muro area (After Tani, 2016)

The survey site in the Nishi Araya area is located on the fringe of the Uchinada sand dunes (Figure 15). This area was excavated as a sand extraction site during the 1960s following the reclamation of the former Kahoku Lagoon and was subsequently filled in during the 1970s, remaining so to this day. Nishi Araya elementary school suffered huge damage due to liquefaction and school remains closed until now. Based on past aerial photographs, land records, and geological survey results, it has been determined that the area between Nishi Araya elementary school, which suffered significant liquefaction damage, and Prefectural Road 8 (indicated by the red line in Figure 15) contains a reclaimed layer extending to a depth of approximately 7 meters.

Furthermore, from a borehole investigation conducted in the vicinity of the survey site in August 2023, prior to the disaster, the reclaimed layer (Fs) was found to extend from the surface to around 7.0 meters deep. Below this, a dune layer (Sd) was identified from 7.0 to around 10.0 meters, an alluvial sand layer (As) from 10.0 to 11.3 meters, an alluvial clay layer (Ac) from 11.3 to 27.6 meters, and a diluvial sand layer (Ds) from 27.6 to 33.45 meters.

Muro area is located on the fringe of the Uchinada sand dunes and is presumed to be an area that was reclaimed following the installation of waterways during the reclamation of the former Kahoku Lagoon (Figure 16). Analysis of the historical aerial photographs, land records, and geological survey results, revealed the existence of a reclaimed layer extending to a depth of 1.5 to 4.5 meters in that area. The area on the east side of the Prefectural Road 8 experienced significant liquefaction and lateral flow induced damage. A borehole investigation conducted by the authors after the disaster confirmed the presence of a reclaimed layer (Fs) from the surface to 4.5 meters, a dune layer (Sd1) from 4.5 to 6.7 meters, and an alluvial clay layer (Ac) from 6.7 to 9.5 meters.

2. Investigation Methods

The following remote sensing and in situ investigations were conducted in Nishi Araya and Muro area, where significant damage to low rise buildings were observed due to lateral flow. The objectives of each surveying technique are also indicated in the following.

1. UAV Photogrammetry (Nishi Araya only) and 3D Laser Scanner: to accurately survey a wide area in order to assess the post-liquefaction ground deformation.
2. Portable Dynamic Cone Penetration Test (PDCPT): allows for continuous checking of the hardness and softness of soil.
3. Piezo Drive Cone (PDC) Test: measures pore water pressure in the ground through a dynamic penetration test, and then estimate the N-value and fine content (FC) to evaluate the liquefaction strength of the soil (PDC Consortium, Japan).
4. Screw Driver Sounding (SDS) Test: measures rotational torque and applied load during ground penetration, enabling the classification of soil layers and rough identification of soil types from the test results (Tanaka et al., 2014).
5. Surface Wave Exploration (Muro only): This geophysical method investigates shallow subsurface structures by measuring and analyzing surface waves (Rayleigh waves) artificially generated by hammering on the ground surface (Hayashi et al., 2001).
6. Standard Penetration Test (SPT): (Muro only)

CASE STUDIES ON LIQUEFACTION AND LATERAL FLOW

1. Case Study 1: Field Survey and Results for the Nishi Araya Area

Figure 17 shows the field survey locations conducted in the Nishi Araya area. In the Figure, the yellow-colored circles represent the survey locations, and the blue colored circles represent the locations of

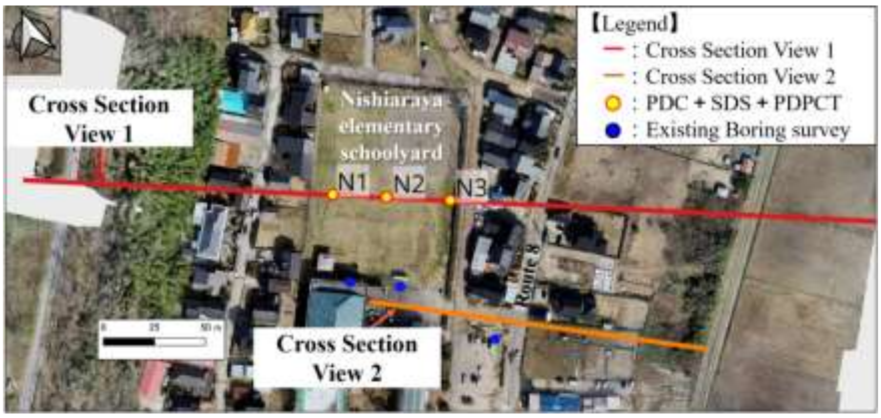

Fig. 17 Field survey locations in the Nishi Araya area

the existing boring survey. Figure 18 shows the 3D point cloud data obtained from the UAV photogrammetry and the field survey results of Nishi Araya area. The UAV photogrammetry confirmed the crack conditions on the playground of Nishi Araya elementary school (red lines), the lateral movement of houses (red ellipses), and the deformation of the Prefectural Road 8 (blue ellipse), which were also identified in the field survey. Additionally, it was confirmed that the crack line corresponds to the location of the excavation site (eventually filled during reclamation) shown in Figure 15.

Fig. 18 Results of UAV surveying and field surveying in the Nishi Araya area

Figure 19 shows a comparison between the pre-disaster topography (5m mesh DEM data of October 5, 2016) obtained from GSI, Japan and the post-disaster topography (Remote sensing data of February 4, 2024) from our 3D laser scanner survey, for the two cross-sections (1 and 2) near Nishi Araya elementary school shown in Figure 17. From cross-section 1, it can be observed that subsidence occurred at the playground of Nishi Araya elementary school (on the Uchinada sand dunes side), where cracks had appeared. However, no change in elevation was detected from the center of the playground to the side of Prefectural Road 8. On the other hand, from cross-section 2, a significant uplift was observed only near the Prefectural Road, while no major topographical changes were detected in the paddy field area toward Kahoku Lagoon.

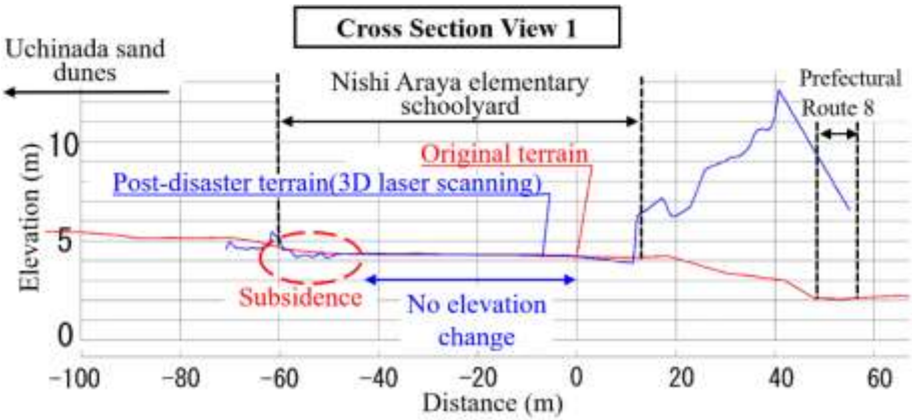

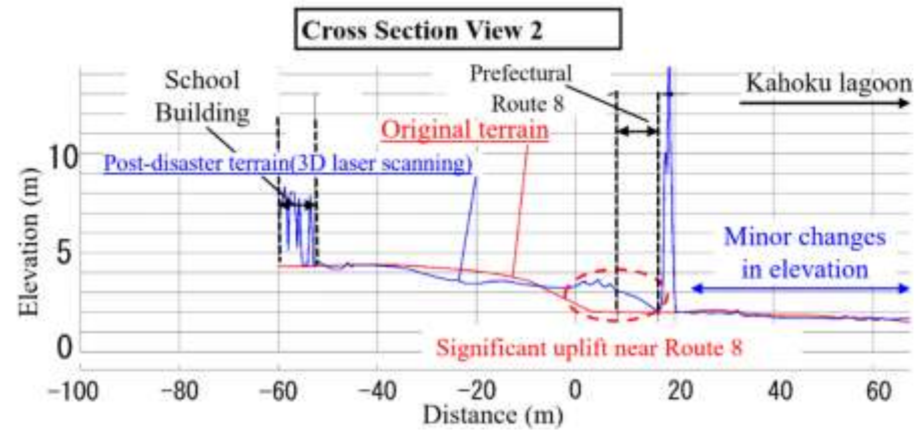

Fig. 19 Comparison between the pre-disaster and post-disaster terrain (3D laser scanning)

The depth profile of the equivalent N-values and fine content Fc at location N1 (see Figure 17), situated at the crack site on the playground of Nishi Araya elementary school, is shown in Figure 20, as representative results from the SDS test, PDC test, and PDCPT. For all the tests, the N-values are below 10 up to a depth of 6 to 7 meters, indicating a loose state of soil post-earthquake. Thereafter, a gradual increase in the N-values with depth can be observed from the PDC and SDS test results. It is to be noted that PDCPT tests were performed only up to a depth of 5 to 7 meters depending on the locations. Furthermore, based on the fine content Fc estimated from the PDC and SDS tests, it is believed that sandy soil with Fc < 50% extends to a depth of approximately 17 meters from the ground surface. The reason for the observed discrepancy in the estimated fine content, Fc between the PDC and SDS test is that, while the PDC test uses only pore water pressure as a parameter to estimate the fines content, the SDS test employs two parameters: torque and applied load. Therefore, when there is little variation in the torque values, the estimated Fc is thought to be strongly influenced by the applied load. Furthermore,

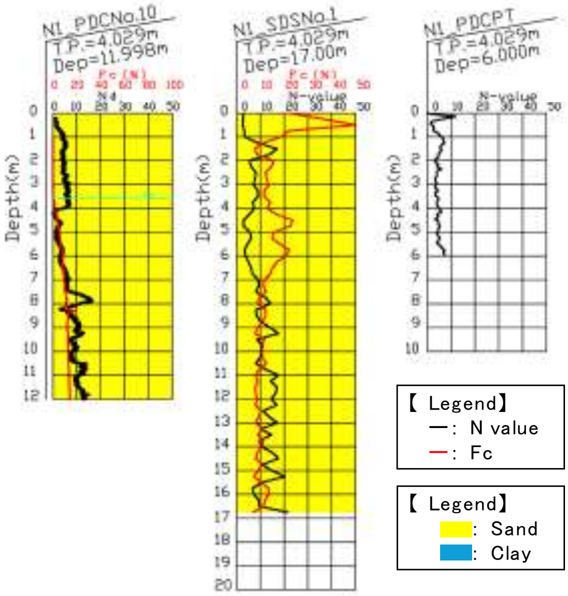

Fig. 20 Comparison among the SDS test, PDC test, and PDCPT results at location N1 in the elementary school's playground

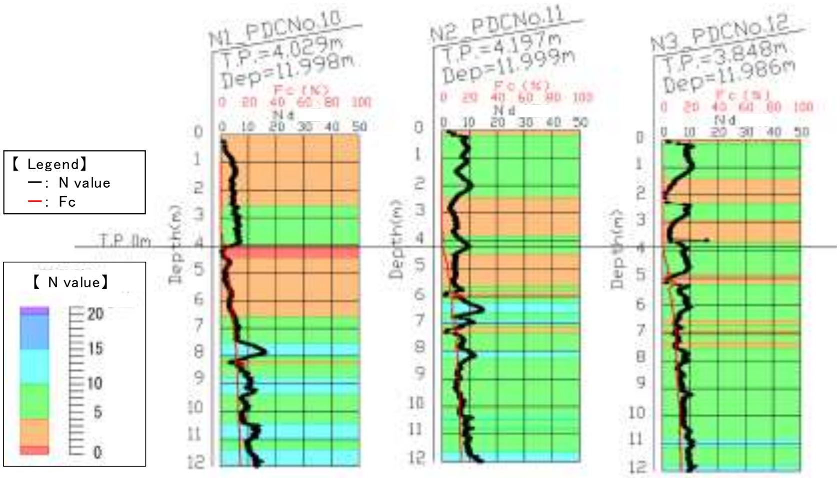

Fig. 21 PDC results at locations N1, N2 and N3 in the elementary school's playground

Figure 21 shows the profile of N-value and fines content with depth obtained from the PDC tests at locations N1, N2 and N3. The results indicate that a loose soil zone with N-values below 5 exists up to a depth of about 6 meters. On the other hand, a very loose soil layer with N-values of 0 to 1 is localized at a depth of around 4 meters towards the Uchinada sand dunes as seen from the penetration data obtained at N1.

2. Case Study 2: Field Survey and Results for the Muro Area

Figure 22 shows the locations of the field survey conducted in the Muro area. In the Figure, locations of the PDC tests, SDS tests and PDCPT are shown in yellow-colored circles, squares, diamonds, triangles and inverted triangles. The light, blue-colored circle (Muro No. 1) represents the location of the Standard Penetration Test (SPT) conducted by the authors, and the dark blue-colored circle represents the location of the existing boring survey. The yellow colored lines represent the locations where the surface wave exploration tests were conducted. In addition, 3-D laser scanning was also conducted in this area. The purpose of selecting these locations was to ascertain the geotechnical and geological characteristics of the Muro area, where a house was displaced by 12 meter due to liquefaction induced lateral spreading (Refer to Figure 10(b)). A pile supported house in the vicinity (Figure 11(a)), however, was not affected by lateral flow.

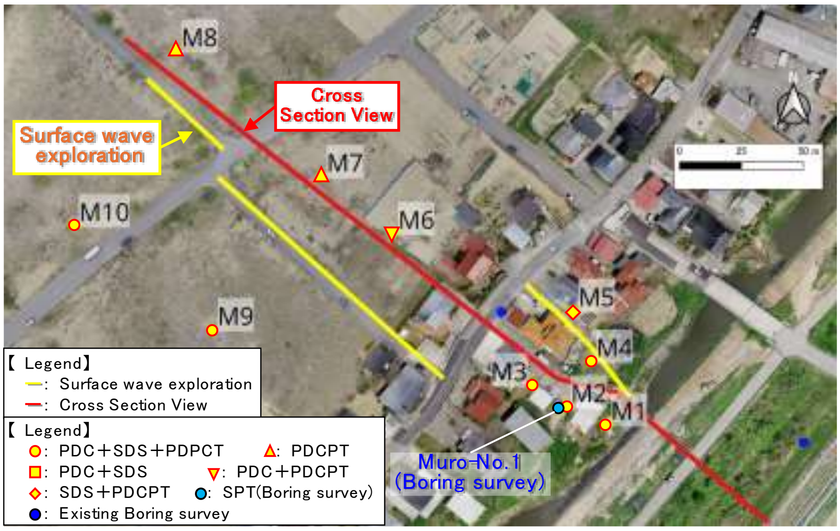

Fig. 22 Field survey locations in the Muro area

Figure 23 shows a comparison between the pre-disaster aerial photographs and point cloud data based on 3D laser scanning taken after the disaster. From the Figure, it could be confirmed that houses located on the east side of the Prefectural Road No. 8, facing the waterway, had shifted approximately 2 to 12 meters toward the waterway. Additionally, the surrounding ground of these houses also moved toward the waterway, displacing the waterway over a distance of approximately 110 meters, and in some areas, nearly blocking the majority of the waterway. On the other hand, no significant movement was observed for houses located on the mountainside (Uchinada sand dunes side), including those along the Prefectural Road No. 8.

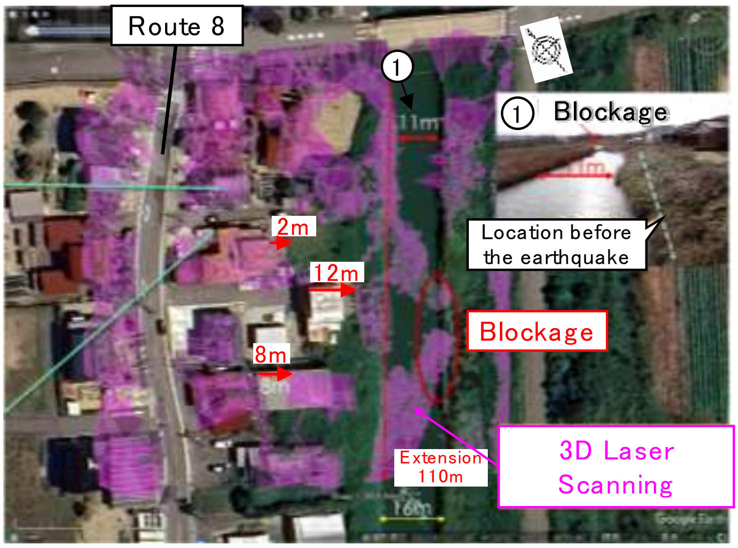

Fig. 23 Comparison of 3D laser scanner survey results (after the disaster) and aerial photographs (before the disaster) in the Muro area

At the location with the largest lateral displacement, a comparison was made between the pre-disaster topography (5m mesh DEM data of October 5, 2016) represented by red line, and the post-disaster topography (Remote sensing data of February 4, 2024) represented by blue line as shown in Figure 24. From this figure, it was found that the maximum lateral displacement of the ground during liquefaction induced lateral spreading was approximately 20 meters, which blocked most part of the waterway. Additionally, the ground surface also was found to experience a maximum settlement of about 1.4 meters. In contrast, it was confirmed that there was little to no change in ground elevation on the west side of the Prefectural Road 8.

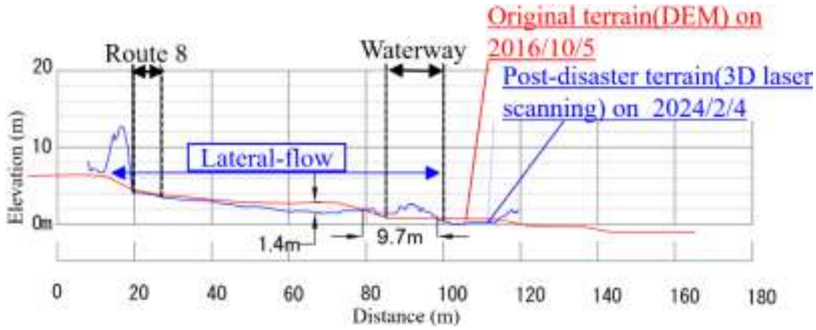

Fig. 24 Comparison between existing topographic data (GSI) and 3D laser scanner survey results

Figure 25 shows the depth profiles of the equivalent N-values and fine content, Fc at location M2 (refer to Figure 22), where sand boils were observed, as the representative test results of the SDS test, PDC test, and PDCPT. All the test results indicated equivalent N-values of 0 to 1 at a depth of approximately 2 meters, indicating an extremely loose soil condition. The reason that the N-values obtained from SPT at a depth of around 2 meters are higher than the equivalent N-values of SDS and PDC is that the SPT was conducted four months later than the other tests, suggesting that the ground stiffness may have recovered by that time. Additionally, below the depth of 2 meters, the equivalent N-values gradually increase to around 20 until about 6 meters deep, after which a decrease in equivalent N-values and an increase in fine content, Fc are observed at around 8 meters.

Based on the comparison as described above, zoning of the N-values was conducted using the depth profiles of N-values and fine content, Fc obtained from the PDC test along the cross section, and is shown in Figure 26. For soil classification, areas with low N-values and fine content, Fc of 50% or more were determined to be clayey soil and the results are depicted in the geological cross-section shown in Figure 27.

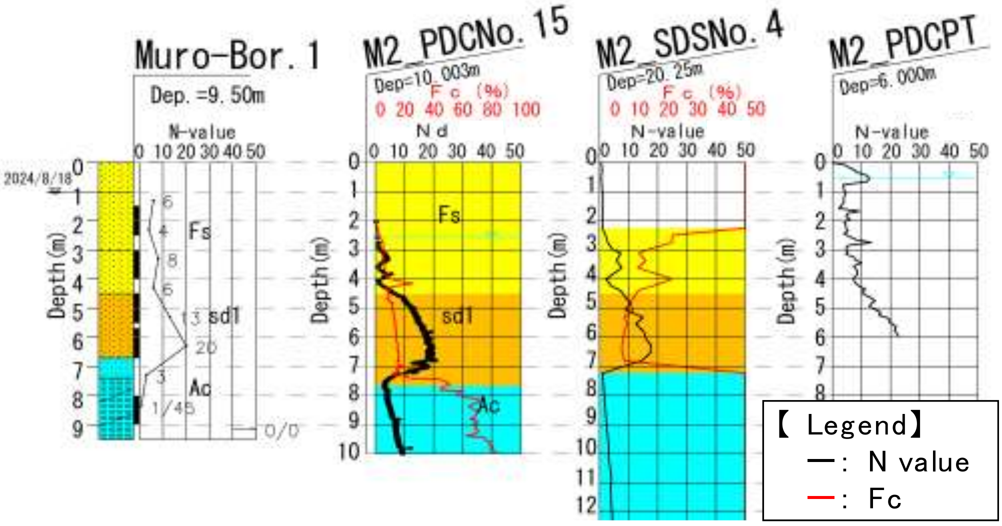

Fig. 25 Comparison of N value and fine content, Fc at a representative location (M2)

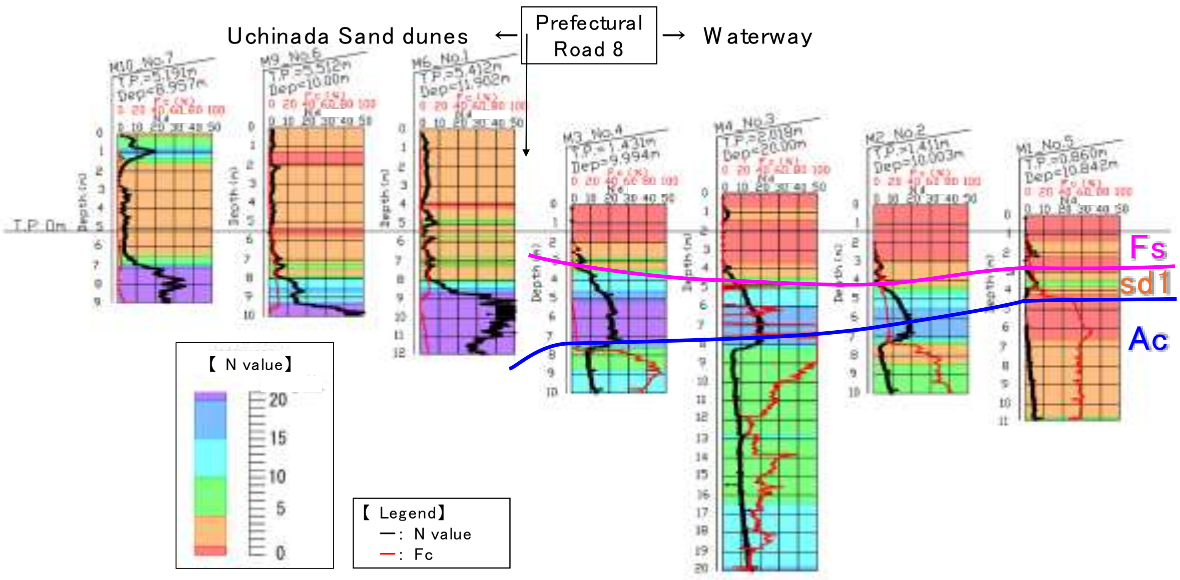

Fig. 26 PDC test results in the cross section

As described before, the Muro area is a reclaimed land by filling the edge of the sand dunes facing Kahoku Lagoon with sandy soil. Very loose zones with N-values of 0 to 1 can be continuously observed in the range of approximately 2 to 4 meters deep on the waterway side (east side) of Prefectural Road 8, where the fill layer is distributed. On the other hand, on the mountainside (west side) of the road, where the sand dunes are located, although there are localized areas with N-values of 0 to 1, continuity of such trend was not observed.

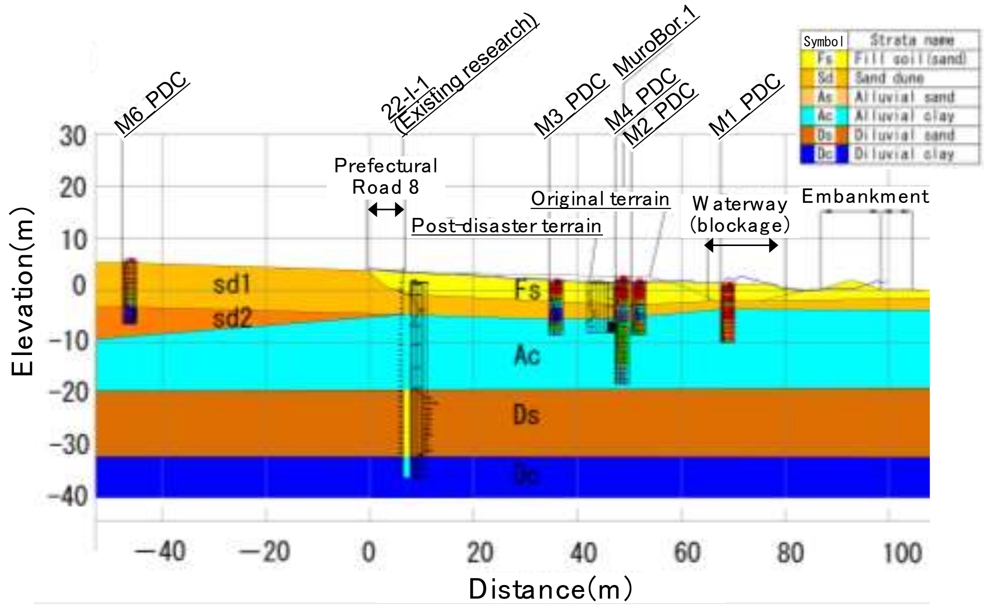

Fig. 27 Estimated geologic cross section obtained from PDC test

The cross-sectional diagram of the S-wave velocity (Vs) obtained from surface wave exploration is shown in Figure 28. Looking at the distribution of S-wave velocities, the region located on the mountainside (sand dunes side) of Prefectural Road 8, has S-wave velocities ranging from 100 to 180 m/s, while the region on the waterway side of the road has a low S-wave velocity of less than 100 m/s. This area roughly corresponds to the fill layer Fs and the very loose area (N-values of 0 to 1) confirmed in the PDC test. The relatively low S-wave velocity of the fill layer Fs, which was filled with dune sand, is thought to be due to the land reclamation that was undertaken in the 1930s, and more likely the fill was not properly compacted.

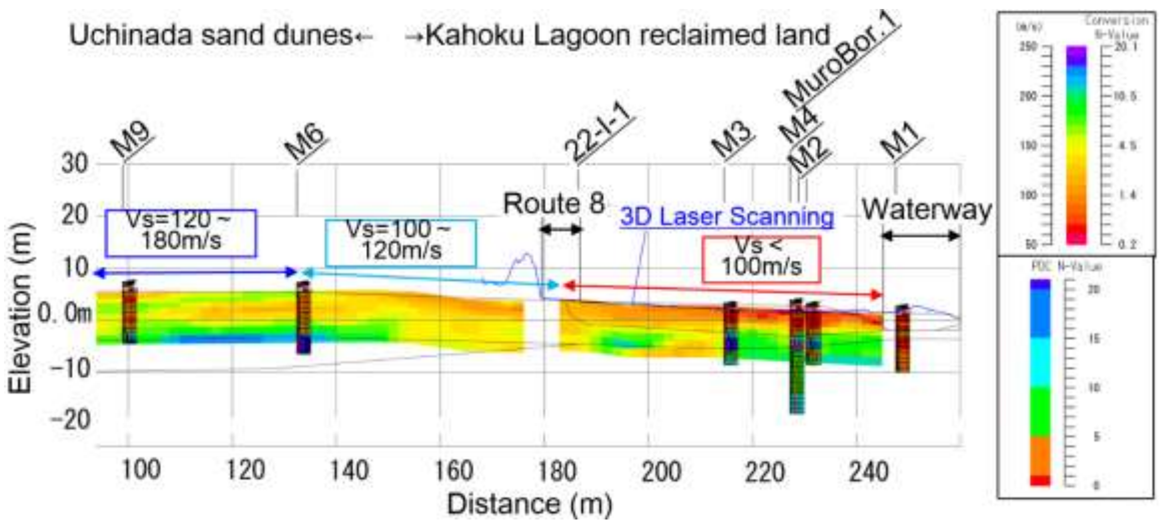

Fig. 28 Result of surface wave exploration survey in the Muro area

Next, focusing on the differences in S-wave velocity within the fill layer Fs, it is particularly noted that there are localized areas with low S-wave velocities near the waterway. Near the waterway, liquefaction-related sand boils and lateral flow that caused blockages have been observed. It can be presumed that, in this area, the lateral flow associated with liquefaction has led to looseness and a decrease in shear stiffness of soils. The boundary between the fill layer and the sand dunes (natural ground) is assumed to be near the Prefectural Road 8. However, examining the distribution of S-wave velocities reveals a region where S-wave velocities range from 100 to 120 m/s, extending approximately 40 meters from the edge of the fill layer. The site exhibits features such as tensile cracks and step-like terrain, indicating a flow slide. This suggests that the area may have undergone secondary slope movement due to lateral flow of the fill layer, Fs.

DISCUSSION ON THE RESULTS

In the areas affected by liquefaction in Uchinada Town, particularly in Nishi Araya and Muro, where significant lateral movement was observed, PDC test, SDS test, PDCPT, and surface wave exploration were conducted to assess the ground's hardness and soil classification. The following conclusions could be made based on the field test results.

1. In the Nishi Araya area, loose zones with N-values below 5 can be observed overall up to a depth of approximately 6 meters. Additionally, a very loose area with N-values of 0 to 1 is localized at a depth of around 4 meters on the Uchinada sand dune side.
2. In the PDC test, zoning of N-values was performed based on the depth profile of the obtained N-values and fine content, Fc. For soil classification, areas with low N-values and fine content Fc of 50% or more were classified as the clayey soil and delineated in the cross-sectional diagram.
3. In the Muro area, very loose zones with N-values of 0 to 1 were continuously observed on the waterway side of Prefectural Road 8, extending to a depth of approximately 2 to 4 meters. In contrast, on the mountainside of Prefectural Road 8, although localized areas with N-values of 0 to 1 exist, continuity was not observed.
4. In the surface wave exploration, the area on the mountainside (west side of Prefectural Road 8) has S-wave velocities ranging from 100 to 180 m/s, whereas the area on the waterway side of the road shows lower S-wave velocities (less than 100 m/s). This area generally corresponds to the fill layer, Fs with very loose sand (N-values of 0 to 1), which was confirmed in the PDC test.
5. The results of the series of ground investigations suggest that liquefaction possibly have occurred at a very shallow depth (approximately 1 to 3 meters from the ground surface) in the Muro area, causing extensive damage in that area.

CONCLUSIONS

The following conclusions could be made based on the two case studies on liquefaction induced later flow.

1. The boring survey results showed that the fill material in the investigation area consists of fine sand. Additionally, the cutting of sand dunes during land reclamation raised the groundwater level, creating conditions favorable for liquefaction.
2. Ground investigations also suggest that liquefaction may have occurred at a shallow depth of approximately 2 to 3 meters.
3. Surface wave exploration in the study area revealed that the east side of Prefectural Road No. 8 has extremely low S-wave velocities (less than 100 m/s). This corresponds to a very loose fill layer (sand with N-values of 0 to 1), as confirmed by the PDC test.
4. Both existing boring data and the geological cross-section from the PDC test identified a 15 meter thick alluvial clay layer at about 6 meters depth. The amplification of seismic waves through this layer is also thought to be a key factor in the widespread liquefaction.
5. In the gently sloping terrain of the Muro area, liquefaction possibly have occurred at shallow depths (within 1 to 3 meters from the surface), causing significant damage due to lateral spreading. The lack of prominent manhole uplift in Uchinada Town too suggests that liquefaction likely occurred at these shallow depths.
6. In the house, whose foundation was supported by improved piles, voids formed beneath the foundations due to liquefaction, however, no differential settlement or lateral movement of the house was observed.
7. Prefectural Road 8 acted as a barrier against lateral spreading, resulting in the uplift of ground along the west side of the road. It is believed that the ground beneath the pavement became compacted and hardened over time due to traffic loads, which helped to suppress the lateral spreading.

A comprehensive investigation on groundwater levels, selection of sites for lowering groundwater based on detailed ground surveys, improvement of the existing liquefaction hazard maps using extensive geological data, and the implementation of cost-effective ground improvement techniques in high-risk areas are among the key challenges that must be addressed to prevent liquefaction induced damage in the area during the future earthquakes.

ACKNOWLEDGEMENT

The authors would like to express their sincere gratitude for the financial supports provided by the President's Special Research Fund of Kyushu University and the Institute of Mathematics for Industry (IMI), Kyushu University. We also wish to acknowledge the generous cooperation of the Department of Education and the Department of Construction, Uchinada Town, during the course of our investigation. Special appreciation is extended to Mr. Shinpei Taniguchi, Mr. Tomonari Ohyama and Ms. Rui Takahashi of Yoshimitsugumi Inc., Komatsu; Dr. Chengjiong Qin of IMAGEi Consultant, Tokyo; Mr. Yoshikazu Ochi of Kawasaki Geological Engineering Co., Ltd., Kyushu Branch; and Mr. Yutao Hu of Kyushu University, Fukuoka for their significant assistance during the field tests and data analysis. The authors would like to express their sincere gratitude to Prof. Emeritus, Takaji Kokusho of Chuo University, Tokyo for his valuable and constructive suggestions throughout the course of this study. Lastly, the authors would like to express their deep gratitude to Mr. Kaoru Mizuno of Uchinada Town, for his generous support in facilitating the field survey and providing essential information throughout our investigations.

REFERENCES

1. Fire and Disaster Management Agency (2024). "Damage Caused by the 2024 Noto Peninsula Earthquake and Response Status of Fire Departments, etc." *(109th report)] Retrieved 16 October 2024.* [in Japanese].
2. Fuji, N. (1971). "Chronology and Paleoenvironmental Condition for the Formation of the Buried Humus Soils of the Coastal Sand Dunes Area in the Hokuriku District, Central Japan", *The Quaternary Research, Journal of Japan Association for Quaternary Research*, Vol. 10, No. 3, pp. 134-146 [in Japanese].

3. Fujishiro, T., Hazarika, H., Matsumoto, T. and Ishizawa, T. (2024). "Overview of Liquefaction Damage in Kahoku City and Uchinada Town due to the 2024 Noto Peninsula Earthquake- (Part 1)", *In: 59th Annual Conference of Japanese Geotechnical Society, Asahikawa, Japan, paper ID: [23-12-2-06]*. [in Japanese].
4. Geospatial Information Authority of Japan (2024). "Landslide and sediment distribution data and map for the 2024 Noto Peninsula Earthquake", *https://www.gsi.go.jp/BOUSAI/20240101_noto_earthquake.html (Accessed: August 8, 2024)*. [in Japanese].
5. Hayashi, K., Suzuki, H. and Saito, H. (2001). "Surface Wave Method using Artificial Sources Development and Application to Civil Engineering Investigations", *OYO technical report 2001*, pp. 9-39. https://www.oyo.co.jp/pdf/technology_annual/2001_03.pdf
6. Hazarika, H., Ishizawa, T., Matsumoto, T., Murai, M., Fujishiro, T., Ohta, S. and Michi, Y. (2024). "Analysis of Liquefaction Damage in Uchinada Town due to the 2024 Noto Peninsula Earthquake", *In: 59th Annual Conference of Japanese Geotechnical Society*, Asahikawa, Japan, paper ID: [25-13-1-04]. [in Japanese].
7. Hu, Y., Qin, C., Hazarika, H., Sahare, A., Kubota, S. and Harima, Y. (2024). "Liquefaction Damage in the Muro District of Uchinada Town due to the 2024 Noto Peninsula Earthquake- (Part 2)", *In: 59th Annual Conference of Japanese Geotechnical Society*, Asahikawa, Japan, paper ID: [25-13-1-02].
8. Japan Meteorological Agency (2024). *https://web.archive.org/web/20240101081217/https://www.data.jma.go.jp/multi/quake/quake_detail.html?eventID=20240101161648&lang=en. Retrieved 16 October 2024*.
9. Kubota, S., Ohta, S., Ochi, Y., Michi, Y., Fujishiro, T., Hazarika, H., Murai, M. and Tanaka, T. (2024a). "Liquefaction Damage in the Muro district of Uchinada Town due to the 2024 Noto Peninsula Earthquake- (Part 3)", *In: 59th Annual Conference of Japanese Geotechnical Society, Asahikawa, Japan, paper ID: [25-13-1-03]*. [in Japanese]
10. Kubota, S., Ohta, S., Hazarika, H., Matsumoto, T., Tanaka, T., Murai, M., Fujishiro, T. and Michi, Y. (2024b). "Investigation Report Siming to Rlucidate the Mechanism of Liquefaction Damage in the Muro District of Uchinada Town due to the 2024 Noto Peninsula Earthquake (Part 1)", *Journal of Japan Society for Natural Disaster (to appear in December 2024)*. [in Japanese]
11. Kubota, S., Ohta, S., Ochi, Y., Imai, T., Hazarika, H., Matsumoto, T., Tanaka, T. and Murai, M. (2024c). "Investigation Report Aiming to Elucidate the Mechanism of Liquefaction Damage in the Muro District of Uchinada Town due to the 2024 Noto Peninsula Earthquake (Part 2)", J*ournal of Japan Society for Natural Disaster (to appear in December 2024)*. [in Japanese]
12. Michi, Y., Fujishiro, T., Matsumoto, T. and Hazarika, H. (2024). "Liquefaction Damage in the Nishi Araya Area of Uchinada Town due to the 2024 Noto Peninsula Earthquake (part 2) - Damage Investigation using UAV photogrammetry and 3D laser surveying", *In: 59th Annual Conference of Japanese Geotechnical Society, Asahikawa, Japan, paper ID: [23-12-2-08]*. [in Japanese]
13. Murai, M., Hazarika, H., Matsumoto, T., Ohta, S. and Kubota, S. (2024). "Liquefaction Damage in the Muro District of Uchinada Town due to the 2024 Noto Peninsula Earthquake- (Part 1): Topography, Geology, and Geological History", *In: 59th Annual Conference of Japanese Geotechnical Society, Asahikawa, Japan, paper ID: [25-13-1-01]*. [in Japanese]
14. National Research Institute for Earth Science and Disaster Resilience (2024a). "Source Inversion Analysis of the Noto Peninsula Earthquake (January 1, 2024, 16:10 JST, M7.6) using Strong Motion Records." *https://www.kyoshin.bosai.go.jp/kyoshin/topics/noto_20240101/inversion/inv_index.html*. [in Japanese]
15. National Research Institute for Earth Science and Disaster Resilience (2024b). "Epicentral Distribution and Initial-Motion Focal Mechanisms of Major Events during the 2024 Noto Peninsula Earthquake based on Hi-net Data" *https://www.hinet.bosai.go.jp/topics/noto240101/?LANG=en&m=summary*. [in Japanese]
16. PDC Consortium, Japan: *About PDC, https://www.pdc-cons.jp/en/about-pdc.html*

17. Sahare, A., Qin, C., Hu, Y., Hazarika, H., Matsumoto, T. and Tanaka, T. (2024). "Liquefaction Damage in the Nishi Araya Area of Uchinada Town due to the 2024 Noto Peninsula Earthquake (Part 2) – Insights from the Nishi Araya elementary School", *In: 59th Annual Conference of Japanese Geotechnical Society, Asahikawa, Japan, paper ID: [23-12-2-07]*.
18. Senna, S. (2024). "Distribution and Characteristics of Liquefaction Damage", *In: Proceedings of the Symposium on the 2024 Noto Peninsula Earthquake, National Research Institute for Earth Science and Disaster Resilience, https://www.bosai.go.jp/introduction/kyoso/kenkyukai/houkokukai_20240305.html*.
19. Tanaka, T., Suemasa, N., Katada, T. and Yamato, S. (2014). "Evaluation of Soil Liquefaction Potential by Screw Driving Sounding Test", *In: Proc. of the Intl. Offshore and Polar Engineering Conference*, pp. 676-681.
20. Tani, K. (2016). "Development of the Konjyaku Map: Distributing and Browsing Service on Old Topographic Map Tiles Images", *Theory and Applications of GIS*, Vol. 25, No. 1, pp. 1-10. [in Japanese].
21. United States Geological Survey (USGS) *https://earthquake.usgs.gov/earthquakes/eventpage/us6000m0xl/executive. Retrieved 16 October 2024*.